



Published in final edited form as:

Clin Radiol. 2018 April ; 73(4): 415.e1–415.e7. doi:10.1016/j.crad.2017.11.007.

Characterisation of meta-analytical functional connectivity in progressive supranuclear palsy

F. Yu^{a,*}, D.S. Barron^b, B. Tantiwongkosi^c, M. Fox^d, P. Fox^d

^aDepartment of Radiology, Massachusetts General Hospital, 55 Fruit St, Boston, MA 02114, USA

^bDepartment of Psychiatry, Yale School of Medicine, 333 Cedar St., New Haven, CT 06510, USA

^cDepartment of Radiology, University of Texas Health Science Center at San Antonio, 7703 Floyd Curl Dr, MC 7800, San Antonio, TX 78229, USA

^dResearch Imaging Institute, University of Texas Health Science Center at San Antonio, 8403 Floyd Curl Dr, San Antonio, TX 78229, USA

Abstract

AIM: To characterise the meta-analytical functional connectivity patterns in progressive supranuclear palsy (PSP) and compare them to idiopathic Parkinson's disease (IPD).

MATERIALS AND METHODS: It was previously reported that PSP and IPD showed distinct regions of brain atrophy based on voxel-based morphometry (VBM) meta-analysis. Using these regions as seeds, healthy control data were referenced to create and statistically compare meta-analytical functional connectivity maps of PSP and IPD.

RESULTS: Some overlap was noted between the two diseases, including within the thalamus, striatum, and prefrontal cortex; however, the PSP seeds demonstrated more extensive functional co-activity throughout the brain, particularly within the midbrain, precentral gyrus, parietal cortex, basal ganglia, and cerebellum.

CONCLUSION: These findings may help guide future longitudinal studies in the development of new functional imaging biomarkers for diagnosis and assessing treatment response.

Introduction

Progressive supranuclear palsy (PSP) is a neurodegenerative tauopathy associated with neurofibrillary tangles and ballooned argyrophilic neuronal degeneration in the basal ganglia, brainstem, and frontal lobes.¹ Patients classically present with Parkinsonian features, followed by the development of vertical gaze palsies, postural instability, dysarthria, and cognitive impairment.² Compared with idiopathic Parkinson's disease (IPD), those afflicted with PSP deteriorate more rapidly (mean survival of 8 versus 15 years), and show little response to levodopa and deep brain stimulation therapy.³ In lieu of these clinical

*Guarantor and correspondent: F. Yu, Department of Radiology, Massachusetts General Hospital, 55 Fruit St, Boston, MA 02114, USA. Tel.: +1 617 726 8323; fax: +1 617 724 3338. frankfy21@gmail.com (F. Yu).

Appendix A. Supplementary data

Supplementary data related to this article can be found at <https://doi.org/10.1016/j.crad.2017.11.007>.

differences, as well as the necessity of appropriately assigning patients in clinical trials, distinguishing these diseases is of great importance.

Although clinical criteria exist, the diagnosis of PSP can be challenging especially in early-stage disease. Structural neuroimaging has shown promise as a diagnostic tool, including manual measurements and semi-automated techniques such as voxel-based morphometry (VBM).^{4,5} Regions of atrophy have been reported within the thalamus, midbrain, striatum, superior cerebellar peduncles, and pre-frontal cortex (PFC)^{6,7}; however, a potential limitation of this approach is that atrophy may not be apparent in early and pre-clinical disease.⁸ Additionally, the significance of these findings and their relationship with clinical impairment remains to be elucidated.⁹

An alternative approach is to focus on the relationship between different brain regions, with an interest in changes to the underlying connectivity. Structural connectivity, representing integrity of white matter tracks, may be evaluated with diffusion imaging, whereas functional connectivity can be assessed through functional MRI (fMRI). Along these lines, there is growing opinion that neurodegenerative disorders, including PSP, may be characterised using a network-based paradigm.¹⁰

Coordinate-based neuroimaging meta-analyses represent a rapidly evolving field, and has been applied to VBM as well as fMRI datasets.^{11–13} As the number of peer-reviewed publications has grown, so has the statistical power of this analytical approach. This has made it possible to identify coactivation patterns across a large number of studies, deriving a meta-analysis of functional connectivity for a user-specified region of interest. A VBM meta-analysis recently reported characteristic atrophy patterns in PSP and IPD.¹⁴ The next step towards defining a robust imaging biomarker for PSP is to evaluate the functional connectivity of these atrophy regions and how these co-activation profiles differ between PSP and IPD. The purpose of the present study was to (1) determine the meta-analytical functional co-activation patterns of the VBM meta-analysis results for PSP and (2) to contrast these co-activation patterns with those of IPD.

Materials and methods

Institutional review board approval was waived as no identifying information or primary patient data were acquired for this study.

Meta-analytical connectivity modelling (MACM)

MACM is based on the concept that whole-brain activation patterns across studies can identify regions with above-chance covariance. This is similar to resting state fMRI (rsfMRI), which uses temporal co-variations in regional activation to detect functional connectivity.^{13,15,16} In MACM, consistent co-activations between two separate brain regions across different fMRI studies may be thought of as the meta-analytical correlate of functional connectivity.¹⁷ This approach overcomes some of the challenges facing individual task-based fMRI studies, including task specificity, low signal-to-noise ratio, and competing network activities.

First, seed regions were derived based on previous VBM meta-analysis of grey matter atrophy in PSP and IPD.¹⁴ This included the left inferior frontal gyrus (IFG), thalamus, midbrain, insula, left claustrum, anterior cingulate cortex (ACC), and left caudate body for PSP. For IPD, these included the bilateral IFGs, left medial frontal gyrus, left superior temporal gyrus, and right middle frontal gyrus (MFG). A search was then conducted of the BrainMap database (which stores coordinate-based results of over 13,000 fMRI experiments) for whole-brain task-based fMRI experiments in healthy subjects demonstrating activations within the seed regions.^{18,19} To avoid pre-selection bias and enable a data-driven approach, all eligible studies were considered regardless of behavioural categories.

Activation likelihood estimation (ALE) meta-analyses were then performed on the coordinates that were identified as coactivating with the seed regions using GingerALE (version 2.3.2). As previously described, the ALE method determines the above-chance convergence between studies, which can be generalised to experiments outside of the current analysis.^{12,14} A cluster-level threshold $p < 0.05$ was incorporated, along with a permutation threshold of 1,000 and false discovery rate (FDR) of $p < 0.05$, to generate MACM-ALE maps of significant convergence across the BrainMap foci.

To facilitate spatial comparisons of IPD and PSP coactivation patterns, the resultant MACM-ALE images were first transformed into binary data using Mango software.¹⁹ A summarised MACM colour map was then generated, demonstrating the extent to which connectivity was shared among the seed regions for each condition. A different colour was attributed to each voxel value (range 0–7). Anatomical labels were assigned based on the Talairach Daemon in Mango, and the results were overlaid on a standardised T1-weighted brain template for visualisation (Colin 27 Average Brain).²⁰

Contrast analysis

To quantitatively contrast the functional connectivity of PSP to IPD, firstly, separate co-activation maps were generated from the combined seeds of each condition. Next, the voxel-wise differences in ALE scores for the respective MACM maps were calculated. The experiments contributing to either analysis were then pooled and randomly divided into two groups of the same size as the set of contrasted experiments.¹² The voxel-wise ALE scores for these randomly assembled groups were subtracted from one another and recorded. Repeating this process over 10,000 permutations yielded a null distribution of ALE-score differences between PSP and IPD, after which p -values and Z -scores were obtained. A map of true differences was then derived using a voxel-wise family-wise error (FWE) threshold of 0.01.

Conjunction analysis

In order to identify consistent functional connectivity maps showing co-activations in both PSP and IPD, conjunction analyses were performed between the two conditions. For this purpose, the thresholded voxel-wise FWE of 0.01 was calculated for each condition, and the intersection between the connectivity maps of both analyses was found to identify areas with significant shared functional co-activity.

Results

MACM of consistent atrophy in PSP

MACM was performed for each of the PSP atrophy seeds (Fig 1; Electronic Supplementary Material Table S1). The thalamic seed demonstrated co-activity with the ACC and posterior cingulate cortex (PCC), prefrontal cortex (PFC), thalamus, striatum, pre- and postcentral gyrus, superior and inferior parietal lobules, temporal–occipital cortices, and cerebellum. Meanwhile, the insular seeds co-activated with the PFC, striatum, thalamus, insula, pre- and postcentral gyrus, superior and inferior parietal lobules, temporal–occipital cortices, and cerebellum.

The striatum, PCC, PFC, pre- and postcentral gyri, superior and inferior parietal lobules, fusiform gyrus, and cerebellum demonstrated co-activity with the left caudate body seed. Similar co-activation patterns were identified with the ACC seed; however, there was absence of co-activity with the cerebellum, superior and inferior parietal lobules, and precentral gyrus. MACM of the left IFG showed functional co-activation with the striatum, thalamus, insula, PFC, pre and postcentral gyrus, fusiform gyrus, temporal cortex, and cerebellum.

There was overlap in co-activity among the PSP seeds within the thalamus, claustrum, caudate head, putamen, insula, ACC and PCC, PFC, pre- and postcentral gyri, left medial frontal gyrus, superior parietal lobule, inferior parietal lobule, precuneus, left supramarginal gyrus, superior temporal gyrus, middle temporal gyrus, left fusiform gyrus, amygdala, left middle occipital gyrus, left inferior occipital lobe, cerebellar hemispheres and vermis (Fig 2). Of these, the most significant overlaps (shared between six or more seeds) were in the MFG, thalamus, claustrum, insula, precentral gyrus, left medial frontal gyrus, inferior parietal lobule, superior temporal gyrus, fusiform gyrus, and anterior cerebellar vermis.

MACM of consistent atrophy in IPD

MACM was also performed for the IPD atrophy seeds (Fig 2; Electronic Supplementary Material Table S2). The more superiorly situated bilateral IFG seeds (seeds 1 and 6) demonstrated co-activation with the thalamus, basal ganglia, insula, PCC, PFC, SMA, pre- and postcentral gyrus, precuneus, superior and inferior parietal lobules, temporal–occipital cortices, amygdala, and cerebellar vermis and hemispheres. The inferiorly situated left IFG seed (seed 4) functionally co-activated with the thalamus, PFC, precentral gyrus, temporal cortices, amygdala, and left posterior cerebellum.

The three medial frontal gyrus seeds demonstrated distinctive functional co-activation patterns. The more inferior seed (seed 2) co-activated with the orbitofrontal PFC only. On the other hand, the two superior seeds (seeds 3 and 7) showed co-activity with the thalamus, caudate, ACC and PCC, insula, PFC, temporal cortices, and amygdala. The right MFG seed co-activated with the thalamus, striatum, midbrain, ACC, PCC, insula, PFC, pre- and postcentral gyrus, precuneus, inferior parietal lobule, temporal cortices, and anterior vermis.

There was significant overlap in functional connectivity within the thalamus, insula, caudate head, putamen, right claustrum, ACC and PCC, MFG, left medial frontal gyrus, IFG, left

superior frontal gyrus, precentral gyrus, amygdala, superior temporal gyri, left fusiform gyrus, middle temporal gyri, inferior parietal gyri, left post central gyrus, right precuneus, right superior parietal lobule, and cerebellar hemispheres and vermis (Fig 3). Among these, the regions with the greatest overlap in co-activity (between five or more seeds) were the thalamus, left medial frontal gyrus, left IFG, right superior temporal gyrus, and left middle temporal gyrus.

PSP versus IPD MACM

Conjunction analysis revealed overlap between the IPD and PSP thresholded co-activation maps in the thalamus, striatum, PCC, PFC, medial frontal gyrus, as well as bilateral parietal and temporal cortices (Fig 4; Electronic Supplementary Material Table S3). Comparing the coactivation maps of the two conditions, the PSP MACM map demonstrated greater functional co-activation within the midbrain, caudate body, ACC, left SFG, precentral gyrus, parietal (BA 7, 40) and temporal (BA 22, 37, 42) cortices, and cerebellum (hemispheres and vermis). In contrast, IPD showed greater co-activation with the PCC, MFG, IFG, anterior temporal lobe (BA 38), amygdala, and para-hippocampal gyrus.

Discussion

MACMs for regions of significant grey matter atrophy in PSP and IPD revealed distinct patterns of functional coactivation based on data from healthy controls. The PSP seeds demonstrated significant overlap in co-activity within the PFC, ACC, temporo-parietal cortices, subcortical grey matter, and cerebellum. Although there was overlap, the PSP seeds showed greater co-activation with the midbrain, striatum, ACC, precentral gyrus, parietal cortex, and cerebellum.

Distinctive meta-analytical connectivity patterns in PSP

Consistent co-activation was identified between the PSP atrophy seeds and the basal ganglia as well as multiple frontal cortical regions, including the PFC, supplemental motor area, premotor cortex, and primary motor cortex. It is known that the thalamus, ACC, and caudate form parallel circuits connecting the basal ganglia and the frontal lobe.²¹ These interconnected networks are involved in motor, cognitive, and autonomic functions; subsequent disruptions may account for the diverse symptoms reported in PSP patients. In particular, disrupted connectivity with the PFC could contribute to deterioration of higher-order cognitive processes (i.e., executive function).

Additionally, significant functional co-activations were found within the parietal cortex, and to a lesser extent the occipital and temporal cortices. It is known that these structures share multiple connections between one another as well as with the frontal cortex and basal ganglia. Correspondingly, complex functions are ascribed to this region including the integration of sensory input, language interpretation, and voluntary movement. It is known that the parietal cortex is involved in voluntary movement, along with the frontal and subcortical motor regions. Several of these posterior regions also comprise nodes of known rsfMRI networks (i.e., default-mode network).¹⁷ Although structural imaging studies

demonstrate relative sparing of these regions in PSP, recent functional studies have reported changes in posterior cerebral activity in diseases that affect the frontal cortex.^{22–25}

Co-activation with the vermis as well as cerebellar hemispheres was demonstrated by the majority of the PSP seeds. Cerebellar involvement has been reported in prior PSP histological and imaging studies.²⁶ Interactions between the cerebellum, thalamus, and frontal cortex have also been established with anatomical pathways between them (i.e., dentatorubrothalamic tract). Conversely, the basal ganglia and cerebellum are traditionally thought of as anatomically and functionally disparate motor centres; however, recent research points to these structures being connected.²⁷ Hoshi *et al.* found di-synaptic connections between both motor and non-motor domains of the dentate with the striatum.²⁸ Interestingly, Burciu *et al.* found increased cerebellar functional activity compared to healthy controls in PSP.²⁵ In this setting, the cerebellum may fulfil a compensatory role in frontal cortical and striatal dysfunction; however, over the course of the disease, cerebellar dysfunction may worsen, contributing to the motor and non-motor symptoms seen in PSP patients.⁹

PSP versus IPD functional connectivity

Previously, grey matter atrophy was noted in PSP to be concentrated within the subcortical structures relative to IPD.^{14,25,29} The present MACM conjunction analysis revealed substantial overlap in their associated co-activation patterns, which may reflect similarities in clinical presentations (i.e., clinical Parkinsonism); however, using contrast analyses, differences in regional co-activity were identified. Although these patterns were derived from healthy control data, they nevertheless highlight areas for further investigation to assess their involvement in pathology and potential utility in diagnosis.

As indicated above, the striatum is involved in voluntary movements through interactions with the frontal lobe. Given the comparatively greater involvement of the deep grey nuclei in PSP based on histopathology and imaging, one may expect associated disturbances of their cortical interactions. Using task-based fMRI, Burciu *et al.* found reduced activity within the basal ganglia as well as motor and premotor cortex in PSP relative to IPD.²⁵ Correspondingly, the PSP subjects in their study also had more severe motor deficits. This observation is supported by FDG-PET imaging, which shows associated decreased metabolism in the frontal lobe, basal ganglia, and midbrain in PSP.²⁹

Differences in frontal cortical–subcortical involvement may account for the variations in higher-order cognitive deficits between the two conditions.²³ Cognitive dysfunction, including clinical dementia, is more prevalent in PSP patients.³⁰ Although both conditions demonstrated PFC connectivity, the PSP seeds had significantly greater co-activity with the dorsolateral PFC, which involves executive functions such as working memory and cognitive flexibility. In particular, there was greater co-activity between the caudate nucleus and PFC—disruption of this interconnection could manifest as impaired cognitive control of complex motor tasks including gait and posture in PSP.^{25,31}

Both PSP and IPD seeds demonstrated co-activations with the parietal and temporal cortex, although PSP exhibited a more extensive posterior distribution.³² More pronounced

changes in functional activity within these cortical regions in PSP compared to IPD patients have also been described using task-based fMRI.²⁵ If present, increased functional activity in these regions could be compensatory to greater striatal dysfunction, driving the recruitment of additional motor circuits to perform movements.^{25,33} The posterior co-activity distribution in PSP was also noted to overlap with the temporoparietal junction and primary auditory regions. Hughes et al. found that network changes in PSP were associated with impaired recognition of emotions in the vocal (auditory) domain.²³ Importantly, disrupted connectivity of these regions may contribute to impaired social cognition, representing a risk factor for further cognitive decline.³⁴

In light of the known structural MRI changes (i.e., atrophy) within the superior cerebellar peduncle and dentate nucleus, PSP was anticipated to have increased meta-analytical functional connectivity with the cerebellum relative to IPD.²⁶ Recent research points to the cerebellum playing an important role in motor-related functions as well as cognition.³⁵ Therefore, disrupted connectivity between cortex, subcortical grey matter, and cerebellum could contribute to the distinguishing clinical features in PSP.

Clinical implications

The present MACM results parallel those from recent PSP rsfMRI studies, which have explored functional connectivity of similar brain regions (e.g., caudate, putamen, and thalamus).^{9,22,26} The correspondence between resting-state functional connectivity networks and MACM co-activation networks has previously been described.^{16,17} Of note, the functional connectivity patterns observed did not precisely correlate with structural imaging findings. The different timescales of BOLD signal and morphological changes (seconds versus months to years) may ensure that only the most robust functional correlations are captured with structural imaging.¹⁶ In the present study, the greatest correspondence between functional and structural covariance (meta-analytical grey matter atrophy) were the subcortical grey matter (i.e., thalamus), ACC, and IFG. These regions could represent critical network “hubs” within the brain, and may be preferentially involved by disease.¹⁰

In addition to diagnosis, a great deal of interest surrounds the role of imaging in predicting clinical progression and therapeutic response. To date, studies investigating the relationship between disease severity and structural metrics (e.g., grey matter atrophy, DTI parameters) in PSP have yielded mixed results.^{9,36} The fact that a better correlation with motor and cognitive function has been reported with functional imaging (i.e., increased or decreased functional connectivity) suggests that clinical disability may reflect disruptions in underlying cortical–subcortical circuits.^{22,26} Therefore, functional imaging may have a role as a biomarker in PSP in the diagnosis of early or preclinical disease, monitoring disease progression, and assessing therapeutic response.

The functional connectivity patterns identified in the present study may potentially be altered or disrupted in their respective diseases. As indicated above, these distinctive networks appear to correspond with the associated clinical manifestations including neuropsychiatric and motor domains; however, additional work is needed to validate these results, with an emphasis on longitudinal studies incorporating primary patient imaging data.

Limitations

The atrophy seeds were derived from meta-analyses of prior VBM studies, which may be influenced by the heterogeneity of the techniques utilised. In particular, segmentation of brainstem nuclei is an area of technical weakness in VBM, which is an important consideration in PSP as well as IPD.³⁷ Additionally, the VBM studies established their diagnoses by clinical criteria. Although these criteria have high sensitivity and specificity for the classic Richardson syndrome, they are not as reliable for other subtypes of PSP. As a consequence, the findings of our meta-analyses cannot necessarily be extended to these groups.

There has been growing interest in characterising white matter changes in neurological diseases using methods such as diffusion tensor imaging as well as VBM.²⁶ For the present study, there were insufficient data to perform a thorough imaging-based meta-analysis of these alternative metrics; however, for future studies, the seed regions employed in the present MACM analysis could also be used to interrogate differences in structural connectivity (based on prospective diffusion tensor imaging data) for PSP and IPD.

Although the motivation for the present study was to explore functional connectivity patterns that could potentially be interrogated for improved early diagnosis, the seeds derived from the previous VBM results were not specific for early disease.¹⁴ Therefore, it cannot be presumed that the present results would be significant in the pre-clinical/early stages. It is also important to note that because MACM is derived from healthy subject data, it serves as a hypothetical model of disease rather than directly characterising disease-related changes.¹⁸ Of note, the possibility that a small subset of individual subjects may have been prodromal for a neurodegenerative disorder cannot be entirely ruled out or controlled for; however, the likelihood that this may significantly contaminate the analysis is minimal: BrainMap meta-analyses of functional connectivity have been consistently shown to predict rsfMRI in healthy controls.¹⁶ Nevertheless, for the reasons stated above, assumptions as to how these connectivity patterns are affected in IDP and PSP patients cannot be made. Previous MACM studies have proven helpful in guiding biomarker development in other neurological diseases (e.g., temporal lobe epilepsy).^{16,38} Therefore, the present results may be best applied as a guide for prospective analyses in primary neuroimaging data.

In summary, distinctive meta-analytical functional connectivity patterns were found for morphometrically defined seeds of structural damage in PSP and IPD. Although there was overlap between the two diseases, PSP demonstrated significantly greater co-activity with the precentral gyrus, parietal cortex, subcortical grey matter, and cerebellum. Disruptions of these proposed networks could potentially account for some of the observed clinical differences between PSP and IPD. Validation of these findings with longitudinal studies of individual subjects is needed, which could help guide the development of new imaging biomarkers for early diagnosis, assessing disease severity, and determining therapeutic efficacy.

Supplementary Material

Refer to Web version on PubMed Central for supplementary material.

References

1. Murray B, Lynch T, Farrell M. Clinicopathological features of the tauopathies. *Biochem Soc Trans* 2005;33(Pt 4):595–9. <https://doi.org/10.1042/BST0330595>. [PubMed: 16042552]
2. Boxer AL, Geschwind MD, Belfor N, et al. Patterns of brain atrophy that differentiate corticobasal degeneration syndrome from progressive supranuclear palsy. *Arch Neurol* 2006;63(1):81–6. 10.1001/archneur.63.1.81 . [PubMed: 16401739]
3. Stamelou M, de Silva R, Arias-Carrion O, et al. Rational therapeutic approaches to progressive supranuclear palsy. *Brain J Neurol* 2010;133(Pt 6):1578–90. 10.1093/brain/awq115.
4. Focke NK, Helms G, Scheewe S, et al. Individual voxel-based subtype prediction can differentiate progressive supranuclear palsy from idiopathic Parkinson syndrome and healthy controls. *Hum Brain Mapping* 2011;32(11):1905–15. 10.1002/hbm.21161.
5. Quattrone A, Nicoletti G, Messina D, et al. MR imaging index for differentiation of progressive supranuclear palsy from Parkinson disease and the Parkinson variant of multiple system atrophy. *Radiology* 2008;246(1):214–21. 10.1148/radiol.2453061703. [PubMed: 17991785]
6. Stamelou M, Knake S, Oertel WH, et al. Magnetic resonance imaging in progressive supranuclear palsy. *J Neurol* 2011;258(4):549–58. 10.1007/s00415-010-5865-0. [PubMed: 21181185]
7. Whitwell JL, Duffy JR, Strand EA, et al. Neuroimaging comparison of primary progressive apraxia of speech and progressive supranuclear palsy. *Eur J Neurol* 2013;20(4):629–37. 10.1111/ene.12004. [PubMed: 23078273]
8. Brun A, Liu X, Erikson C. Synapse loss and gliosis in the molecular layer of the cerebral cortex in Alzheimer's disease and in frontal lobe degeneration. *Neurodegener J Neurodegener Disord Neuroprotection Neuroregeneration* 1995;4(2):171–7.
9. Piattella MC, Tona F, Bologna M, et al. Disrupted resting-state functional connectivity in progressive supranuclear palsy. *AJNR Am J Neuroradiol* 2015;36(5):915–21. 10.3174/ajnr.A4229. [PubMed: 25655870]
10. Seeley WW, Crawford RK, Zhou J, et al. Neurodegenerative diseases target large-scale human brain networks. *Neuron* 2009;62(1):42–52. 10.1016/j.neuron.2009.03.024. [PubMed: 19376066]
11. Eickhoff SB, Laird AR, Grefkes C, et al. Coordinate-based activation likelihood estimation meta-analysis of neuroimaging data: a random-effects approach based on empirical estimates of spatial uncertainty. *Hum Brain Mapping* 2009;30(9):2907–26. 10.1002/hbm.20718.
12. Eickhoff SB, Bzdok D, Laird AR, et al. Activation likelihood estimation meta-analysis revisited. *NeuroImage* 2012;59(3):2349–61. 10.1016/j.neuroimage.2011.09.017. [PubMed: 21963913]
13. Laird AR, Lancaster JL, Fox PT. BrainMap: the social evolution of a human brain mapping database. *Neuroinformatics* 2005;3(1):65–78. [PubMed: 15897617]
14. Yu F, Barron DS, Tantiwongkosi B, et al. Patterns of gray matter atrophy in atypical Parkinsonism syndromes: a VBM meta-analysis. *Brain Behav* 2015;5(6):e00329, 10.1002/brb3.329.
15. Robinson JL, Laird AR, Glahn DC, et al. Meta-analytical connectivity modeling: delineating the functional connectivity of the human amygdala. *Hum Brain Mapping* 2010;31(2):173–84. 10.1002/hbm.20854.
16. Reid AT, Hoffstaedter F, Gong G, et al. A seed-based cross-modal comparison of brain connectivity measures. *Brain Struct Funct* 2017;222(3):1131–51. 10.1007/s00429-016-1264-3. [PubMed: 27372336]
17. Smith SM, Fox PT, Miller KL, et al. Correspondence of the brain's functional architecture during activation and rest. *Proc Natl Acad Sci U S A* 2009;106(31):13040–5. 10.1073/pnas.0905267106.
18. Laird AR, Eickhoff SB, Fox PM, et al. The BrainMap strategy for standardization, sharing, and meta-analysis of neuroimaging data. *BMC Res Notes* 2011;4:349. 10.1186/1756-0500-4-349. [PubMed: 21906305]
19. Fox PT, Lancaster JL. Mapping context and content: the BrainMap model. *Nat Rev Neurosci* 2002;3(4):319–21. 10.1038/nrn789. [PubMed: 11967563]
20. Lancaster JL, Woldorff MG, Parsons LM, et al. Automated Talairach atlas labels for functional brain mapping. *Hum Brain Mapping* 2000;10(3):120–31.

21. Haber SN, Calzavara R. The cortico-basal ganglia integrative network: the role of the thalamus. *Brain Res Bull* 2009;78(2e3):69–74. 10.1016/j.brainresbull.2008.09.013. [PubMed: 18950692]
22. Gardner RC, Boxer AL, Trujillo A, et al. Intrinsic connectivity network disruption in progressive supranuclear palsy. *Ann Neurol* 2013;73(5):603–16. 10.1002/ana.23844. [PubMed: 23536287]
23. Hughes LE, Ghosh BCP, Rowe JB. Reorganisation of brain networks in fronto-temporal dementia and progressive supranuclear palsy. *NeuroImage Clin* 2013;2:459–68. 10.1016/j.nicl.2013.03.009. [PubMed: 23853762]
24. Zhou J, Greicius MD, Gennatas ED, et al. Divergent network connectivity changes in behavioural variant frontotemporal dementia and Alzheimer's disease. *Brain J Neurol* 2010;133(Pt 5):1352–67. 10.1093/brain/awq075.
25. Burciu RG, Ofori E, Shukla P, et al. Distinct patterns of brain activity in progressive supranuclear palsy and Parkinson's disease. *Mov Disord* 2015;30(9):1248–58. 10.1002/mds.26294. [PubMed: 26148135]
26. Whitwell JL, Avula R, Master A, et al. Disrupted thalamocortical connectivity in PSP: a resting-state fMRI, DTI, and VBM study. *Parkinsonism Relat Disord* 2011;17(8):599–605. 10.1016/j.parkreldis.2011.05.013. [PubMed: 21665514]
27. Wu T, Hallett M. The cerebellum in Parkinson's disease. *Brain* 2013;136(3):696–709. 10.1093/brain/aws360. [PubMed: 23404337]
28. Hoshi E, Tremblay L, Feger J, et al. The cerebellum communicates with the basal ganglia. *Nat Neurosci* 2005;8(11):1491–3. 10.1038/nn1544. [PubMed: 16205719]
29. Broski SM, Hunt CH, Johnson GB, et al. Structural and functional imaging in Parkinsonian syndromes. *RadioGraphics* 2014;34(5):1273–92. 10.1148/rg.345140009. [PubMed: 25208280]
30. Tolosa E, Duvoisin R, Cruz-Sanchez FF. *Progressive supranuclear palsy: diagnosis, pathology, and therapy*. Springer Verlag; 2013.
31. Evarts EV, Kimura M, Wurtz RH, et al. Behavioral correlates of activity in basal ganglia neurons. *Trends Neurosci* 1984;7(11):447–53. 10.1016/S0166-2236(84)80151-4.
32. Ghosh BCP, Calder AJ, Peers PV, et al. Social cognitive deficits and their neural correlates in progressive supranuclear palsy. *Brain* 2012;135(7):2089. 10.1093/brain/aws128. [PubMed: 22637582]
33. Yu H, Sternad D, Corcos DM, et al. Role of hyperactive cerebellum and motor cortex in Parkinson's disease. *NeuroImage* 2007;35(1):222–33. 10.1016/j.neuroimage.2006.11.047. [PubMed: 17223579]
34. Hardy CJD, Marshall CR, Golden HL, et al. Hearing and dementia. *J Neurol* 2016;263(11):2339. 10.1007/s00415-016-8208-y. [PubMed: 27372450]
35. Reetz K, Dogan I, Rolfs A, et al. Investigating function and connectivity of morphometric findings—exemplified on cerebellar atrophy in spinocerebellar ataxia 17 (SCA17). *NeuroImage* 2012;62(3):1354–66. 10.1016/j.neuroimage.2012.05.058. [PubMed: 22659444]
36. Whitwell JL, Schwarz CG, Reid RI, et al. Diffusion tensor imaging comparison of progressive supranuclear palsy and corticobasal syndromes. *Parkinsonism Relat Disord* 2014;20(5):493–8. 10.1016/j.parkreldis.2014.01.023. [PubMed: 24656943]
37. Shigemoto Y, Matsuda H, Kamiya K, et al. In vivo evaluation of gray and white matter volume loss in the parkinsonian variant of multiple system atrophy using SPM8 plus DARTEL for VBM. *NeuroImage Clin* 2013;2:491–6. 10.1016/j.nicl.2013.03.017. [PubMed: 24179801]
38. Barron DS, Fox PT, Pardoe H, et al. Thalamic functional connectivity predicts seizure laterality in individual TLE patients: application of a biomarker development strategy. *NeuroImage Clin* 2015;7:273–80. 10.1016/j.nicl.2014.08.002. [PubMed: 25610790]

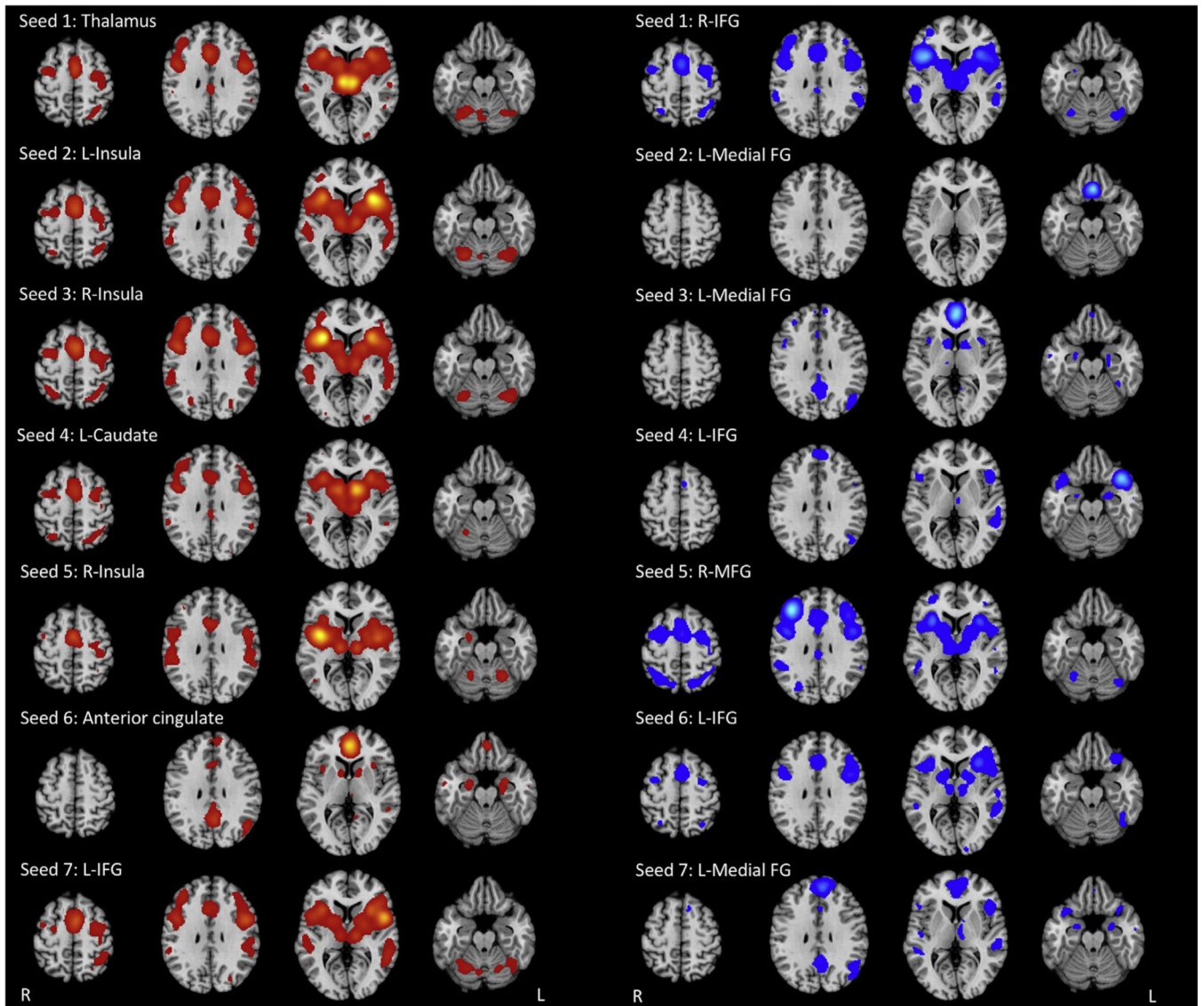


Figure 1. MACM maps derived from healthy control data for each atrophy seed (PSP in red; IPD in blue).

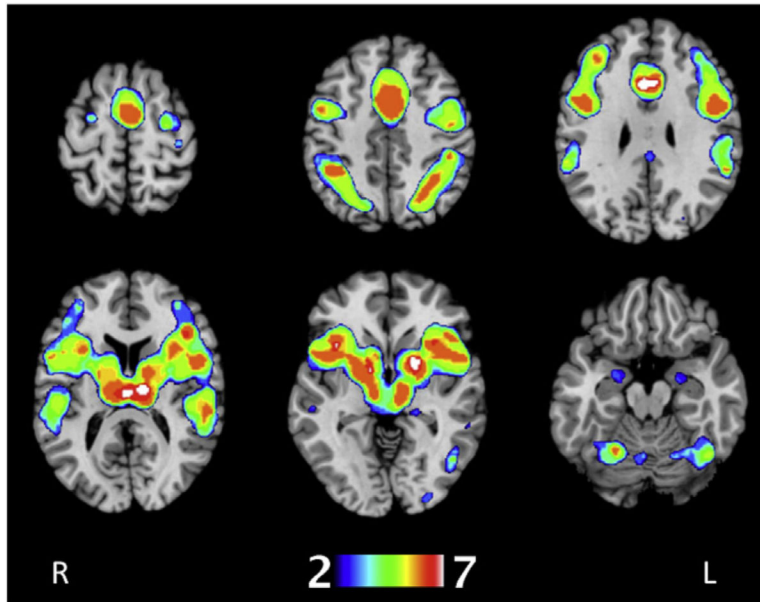


Figure 2. Summarised MACM colour map derived from healthy control data showing areas of meta-analytical functional covariance shared by the seven PSP atrophy seeds. To create these images, ALE cluster maps were binarised and spatially added and overlaid onto the MNI152 brain. The colours range from blue (voxels shared by two seeds) to white (voxels shared by all seven seeds).

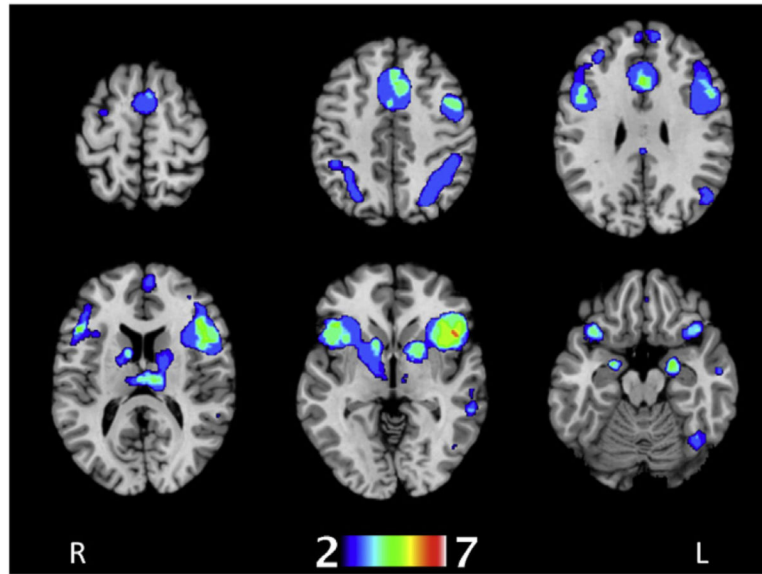


Figure 3. Summarised MACM colour map derived from healthy control data showing areas of meta-analytical functional covariance shared by the seven IPD atrophy seeds. To create these images, ALE cluster maps were binarised and spatially added and overlaid onto the MNI152 brain. The colours range from blue (voxels shared by two seeds) to white (voxels shared by all seven seeds).

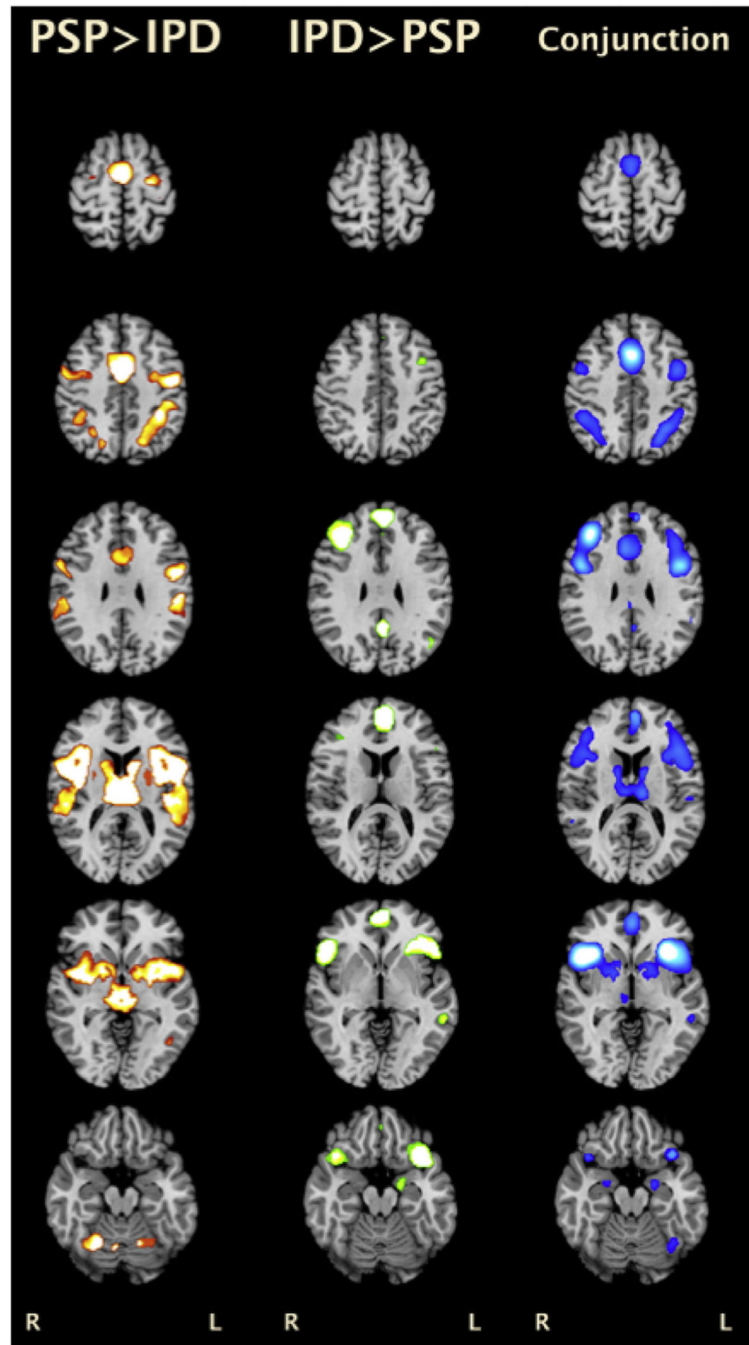


Figure 4. Results of contrast (left two columns) and conjunction analyses (rightmost column) for PSP and IPD MACM. All results were thresholded at a voxel-wise FWE of 0.01.